RSC Advances

PAPER

View Article Online
View Journal | View Issue

CrossMark click for updates

Cite this: *RSC Adv.*, 2016, **6**, 98476

Published on 11 October 2016. Downloaded by Fail Open on 7/23/2025 9:11:32 AM.

Zeolite based solid-phase extraction coupled with UPLC-Q-TOF-MS for rapid analysis of acetylcholinesterase binders from crude extract of *Corydalis yanhusuo*†

Yi Tao,*[ab] Yanhui Jiang,[ab] Weidong Li[ab] and Baochang Cai[ab]

A very convenient, sensitive and precise solid-phase extraction approach was established for extract and analysis of acetylcholinesterase binders from crude extract of *Corydalis yanhusuo*. This approach was based on the retention of binders by acetylcholinesterase immobilized zeolite. The retained acetylcholinesterase binders were eluted and analyzed by ultra-high performance liquid chromatography and quadrupole-time-of-flight mass spectrometry. The powder X-ray diffraction (XRD), transmission electron microscopy (TEM), and Fourier transform infrared (FT-IR) spectroscopy techniques were employed for the characterization of acetylcholinesterase immobilized zeolite. Some experimental conditions such as incubation temperature, time, buffer pH and ion strength, which may affect binding capability, were investigated by using coptisine as a model inhibitor. The optimal incubation conditions were as follows: wash times: 4, wash solvent: 50% methanol–water, incubation time: 20 min, temperature: 37 °C, ion strength: 10 mM, pH: 7.4. The proposed approach was successfully applied for the extraction of acetylcholinesterase binders from crude extract of *Corydalis yanhusuo*. These binders were further validated by acetylcholinesterase inhibitory assay. Fourteen acetylcholinesterase inhibitors were identified, and ten of which, including dehydrocorydaline, allocryptopine, corydaline, dehydroglaucine, protopine, tetrahydrocoptisine, tetrahydropalmatine, corynoline, tetrahydrocolumbamne and tetrahydroberberine, were reported for the first time. In addition, the merits and shortcomings of zeolite based solid-phase extraction approach were compared with that of magnetic nanoparticles based solid-phase extraction approach.

Received 2nd October 2016
Accepted 11th October 2016

DOI: 10.1039/c6ra24585d

www.rsc.org/advances

Introduction

The development of convenient and reliable methods for solid-phase extraction of acetylcholinesterase (AChE) binders is a valuable task because AChE plays crucial roles in many biological processes and is a potential biomarker in clinical diagnosis.[1] As a hydrolase, AChE catalyzes the breakdown of acetylcholine and of some other choline esters that function as neurotransmitters. Inhibition of AChE leads to accumulation of ACh in the synaptic cleft and results in impeded neurotransmission. Because of the pivotal role that AChE plays in the nervous system, the enzyme has long been an attractive target for the rational design of mechanism-based inhibitors. Doctors are now willfully poisoning AChE in an attempt to reverse the symptoms of Alzheimer's disease. People with Alzheimer's disease lose many nerve cells as the disease progresses. By taking a drug that partially blocks AChE, the levels of the neurotransmitter can be raised, strengthening the nerve signals that remain.[2]

Corydalis yanhusuo, which is a folk medicine distributed in southeast of China, is employed in traditional Chinese medicines as an analgesic agent for treating spastic pain, abdominal pain, menstrual pain, and pain due to injuries.[3] The major constituents of *Corydalis yanhusuo* were protoberberine-type alkaloids and tetrahydroprotoberberine-type alkaloids.[4] Coptisine, one of the major alkaloids, exhibited significantly inhibitory effects against AChE. Moreover, quaternary ammonium alkaloids of many medicinal plants are important plant metabolites with significant effects on inhibition of neuromuscular transmission.[5] Therefore, it was hypothesized that other AChE inhibitory agents may exist in the plant.

Zeolites are metastable crystalline aluminosilicate molecular sieves with uniform pores of molecular dimensions that are widely applied in catalysis,[6–8] separations,[9] and adsorption.[10] Adsorption is one of the simplest methods to immobilize

[a]*School of Pharmacy, Nanjing University of Chinese Medicine, Xianlin Campus, 138 Xianlin Avenue, Nanjing 210023, PR China. E-mail: taoyi1985812@126.com; Fax: +86-25-86798281; Tel: +86-25-86798281*

[b]*Jiangsu Key Laboratory of Chinese Medicine Processing, Nanjing University of Chinese Medicine, Nanjing, 210023, PR China*

† Electronic supplementary information (ESI) available. See DOI: 10.1039/c6ra24585d

This journal is © The Royal Society of Chemistry 2016

Published on 11 October 2016. Downloaded by Fail Open on 7/23/2025 9:11:32 AM.

enzyme and presents the additional advantage of being a "soft" and inexpensive method. Main advantages of using zeolites as support for enzyme immobilization[11] include (i) the materials typically exhibit high internal surface areas, allowing them to physically adsorb significant amounts of enzymes, (ii) generating a strong but reversible immobilization that enables us to recover expensive enzymes,[12,13] and (iii) providing a possibility to selective separation of immobilized enzymes from a reaction mixture.

In this study, a new approach using AChE immobilized zeolite to solid-phase extraction of AChE binders from crude extract of *Corydalis yanhusuo* was established. A flowchart of the proposed approach is shown in Fig. 1. First, zeolites were immersed into AChE solution and adsorbed AChE onto their surface. Second, the crude extract of *Corydalis yanhusuo* was incubated with AChE immobilized zeolite for an appropriate period. Subsequently, the unbound compounds and nonspecific binding compounds were separated and abandoned, whereas the specific bound compounds were dissociated from AChE immobilized zeolite using organic denaturing reagents. The specific bound compounds were analyzed by ultra-high performance liquid chromatography and quadrupole-time-of-flight mass spectrometry and their activities were validated using AChE inhibitory assay. In addition, the merits and shortcomings of zeolite based solid-phase extraction approach were compared with that of magnetic nanoparticles based solid-phase extraction approach.

Experimental

Chemicals and reagents

Acetylcholinesterase (from *Electrophorus electricus*, EC:3.1.1.7), 5,5′-dithiobis(2-nitrobenzoic acid) and acetylthiocholine were obtained from Sigma Co. Galantamine was purchased from Tianjin Meilun Shengwu Technology Co. Tetrahydrocolumbamine, columbamine, coptisine, berberine, tetrahydrocoptisine, dehydro-corydaline, tetrahydropalmatine, tetrahydroberberine, dehydroglaucine, corydaline, protopine, corynoline and allocryptopine were purchased from Chengdu Herbpurify Co. Palmatine hydrochloride was obtained from Shanghai yuanye Bio-Technology Co. Purities of all the reference compounds were greater than 98%. Three types of zeolites including zeolite Y (Si/Al = 7 : 1), zeolite ZSM-5 (Si/Al = 25 : 1) and zeolite beta (Si/Al = 25 : 1) were obtained from Tianjin Real & Lead Chemical Co. Monodispersed amine functionalized magnetite nanoparticles (1 mg mL^{-1}) were obtained from Tianjin BaseLine ChromTech Research Centre. HPLC-grade acetonitrile was purchased from Merck Co. 96-well microtiter plates were obtained from Corning Inc. All solutions and dilutions were prepared with ultrapure water from a Milli-Q water purification system.

Apparatus

The AChE adsorption device was home-made and intelligent thermostatic water bath were purchased from Jintan Baitaxinbao Instrumental Co. The analytical apparatus used in the current study included a transmission electron microscopy (JEM-2100), a scanning electron microscope (Hitachi S4800), a X-ray diffractometer (XPert PRO), a Fourier transform infrared spectroscopy (Bruker Optics), a vibration sample magnetometer (PPMS-9), a ZetaMaster 3000 zeta potential laser particle size analyzer (Malvern), an Agilent 1100 LC-UV system with chemstation (Agilent), a Shimadzu UPLC system (Shimadzu), a Q-TOF 5600-plus mass spectrometer equipped with Turbo V sources and a TurboIonspray interface (AB sciex), a PB-10 Sartorious pH meter (Sartorious), a Synergy 2 multimode reader (Biotek) and a Milli-Q Water Purification System (Millipore Co).

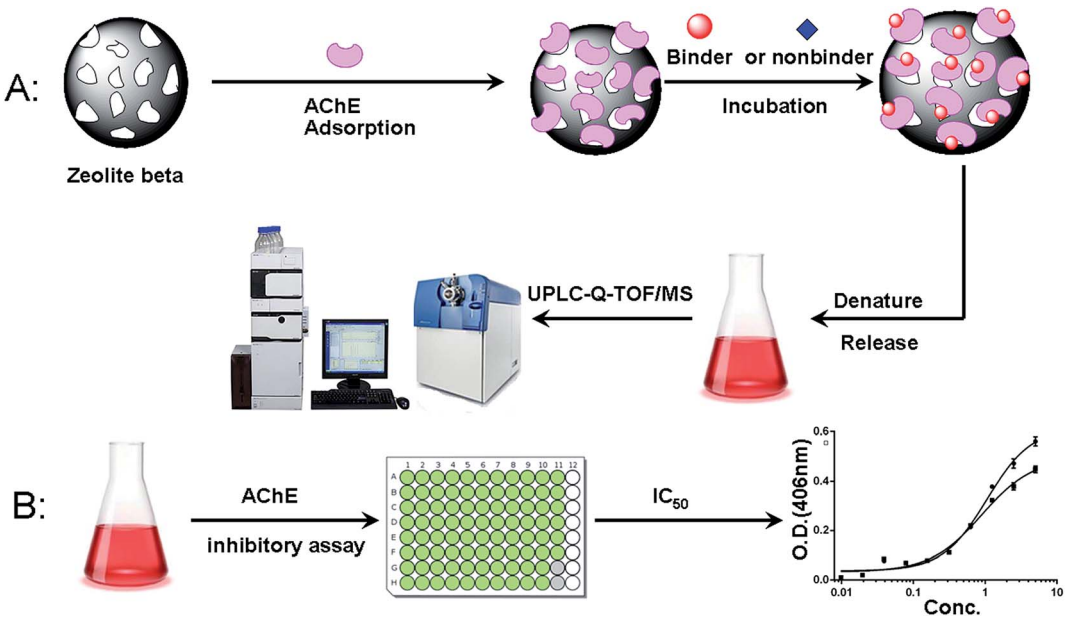

Fig. 1 Schematic diagram of the acetylcholinesterase immobilized zeolite-based solid-phase extraction approach.

Published on 11 October 2016. Downloaded by Fail Open on 7/23/2025 9:11:32 AM.

Preparation of AChE immobilized zeolites and AChE conjugated magnetic nanoparticles

The homemade device used in this study for AChE adsorption is shown in Fig. S1.† All adsorption experiments were conducted at 25 °C. Five milliliters of AChE solution with a given initial concentration (2 mg mL^{-1}) in phosphate buffer solution (200 mM, pH 6.2) was transferred into a homemade glass chamber. Zeolites (5 mg) were immersed into the buffer and then incubated in the AChE solution and shaken gently in a circulating water bath for 30 min. 20 μL aliquot of incubation solution from the chamber was taken regularly and assayed for protein content using the Bradford method.

Three parameters were investigated in the current study to optimize the adsorption procedure. First, experiments with different kinds of zeolites (*i.e.* zeolite Y, zeolite ZSM-5 and zeolite beta) and a constant amount of AChE (5 mL, 2 mg mL^{-1}) were performed to study the amount of protein efficiently immobilized on the zeolites. Samples of the supernatants were withdrawn and the amount of entrapped protein on the zeolites was calculated from the protein mass balance among the initial and final AChE solutions. Second, PBS solutions with different pH values (5.8, 6.2, 6.8, 7.2 and 8.0) were investigated. Third, different temperatures (25, 30, 37 and 45 °C) were used to study the influence of temperature on the adsorption efficiency. Analysis of variance was used to assess the results.

Recovery of AChE from adsorbents under certain conditions is an important issue. Therefore, desorption behavior of AChE from zeolites was also performed. Prior to the desorption experiment, AChE solution and zeolites were incubated at room temperature, because the adsorption equilibrium of the AChE on zeolites was sufficiently reached around 45 min under this experimental condition. The mixtures were centrifuged to obtain zeolite-adsorbed fractions which include zeolites and adsorbed AChE. Then, zeolite-adsorbed fractions were washed three times with fresh buffer to exclude non-specific and weakly adsorbed AChE. Desorption of AChE adsorbed on zeolites was performed by addition of 0.2 M NaOH solutions to the zeolite-adsorbed fraction. The mixture of NaOH solution and zeolite-adsorbed fraction was incubated for 45 min at 37 °C. Supernatant was obtained by flash spin down at 12 000 rpm for several seconds. Concentration of desorbed protein in supernatant was determined by Bradford method. Meanwhile, the pH of desorbed protein solution was adjusted to 7.0 by adding HCl solution. Then, the protein solution was freeze-dried to obtain protein powder. The activity of the desorbed protein powder was compared with that of original protein powder.

The conjugation of AChE onto amine-terminated magnetic nanoparticles was performed by a typical glutaraldehyde activation procedure. 25 μL amine-terminated magnetic nanoparticles were suspended in 120 μL 1% glutaraldehyde for 1 h. The amine-terminated magnetic nanoparticles were recovered by magnetic separation and washed three times with phosphate buffer solution to remove excess glutaraldehyde. Then, the amine-terminated magnetic nanoparticles was suspended in AChE solution (1.0 mg mL^{-1}, dissolved in phosphate buffer solution) and shaken for 2 h at 25 °C, after which, the AChE conjugated magnetic nanoparticles was recovered by magnetic separation and thoroughly rinsed with phosphate buffer solution three times to remove unbound AChE. Experiments with varying amounts of magnetic nanoparticles (25, 50, 75, 100, 125, 150 and 175 μL) and a constant amount of AChE (100 μL, 1 mg mL^{-1}) were performed to study the amount of protein efficiently immobilized on the magnetic nanoparticles. The supernatant and three wash solutions were kept in order to determine AChE loading efficiency by Bradford method. The AChE conjugated magnetic nanoparticles were dispersed in phosphate buffer solution and stored at 4 °C for further experiments.

Morphology characterization

Powder X-ray diffraction (PXRD) data of zeolites were collected on a PANalytical X'Pert PRO diffractometer in the Bragg–Brentano geometry using CuKα radiation. The morphologies of AChE immobilized zeolites and AChE conjugated magnetic nanoparticles were determined by transmission electron microscopy (TEM). Fourier transform infrared spectroscopy (FTIR) was acquired on a Bruker infrared spectrometer. Magnetization curves of magnetic nanoparticles were measured in a vibration sample magnetometer. Hydrodynamic sizes and zeta potential were detected using zeta potential laser particle size analyzer.

Sample preparation

The rhizome of *Corydalis yanhusuo* was collected from Jinhua City, Zhejiang Province, and authorized by Prof. Cai Baochang in the field. Voucher specimens were deposited in the herbarium of Jiangsu Key Laboratory of Chinese Medicine Processing, Nanjing University of Chinese Medicine (no. CY150715). The sample preparation procedures were as follows: first, the rhizome of *Corydalis yanhusuo* was pulverized into powder and sieved (60 meshes). Second, an aliquot (1.0 g) of the powder was accurately weighed and refluxed in 50 mL of water for 1 h and then filtered. Third, the filtrate was centrifuged at 13 400 rpm for 10 min and the supernatant was stored in −20 °C for the next experiment.

Optimization conditions for AChE immobilized zeolites based solid-phase extraction

All experiments were performed in 1.5 mL centrifuge tubes. The reactions of the model compound (20 μL, 1 mg mL^{-1} for the standard compound coptisine) and 0.025 mg AChE immobilized zeolites were mixed with phosphate buffer solution (final volume, 200 μL) and incubated at 37 °C for 20 min in a water bath. The AChE immobilized zeolites were washed four times with 200 μL of the buffer and the supernatant was stored. The AChE immobilized zeolites were subsequently washed using 20 μL of 50% (v/v) methanol/water to dissociate specific bound compounds. The eluate was collected and analyzed.

Coptisine exhibited AChE inhibitory activity and was a kind of major alkaloids.[14] Alkaloids were the major constituents of *Corydalis yanhusuo*. The same kind of compounds shared the same characteristics. Therefore, coptisine was selected as a model compound to optimize the extraction condition. Six

 This journal is © The Royal Society of Chemistry 2016

Published on 11 October 2016. Downloaded by Fail Open on 7/23/2025 9:11:32 AM.

parameters were investigated. First, different wash times (one to five times) and different denature solvents including acetonitrile–water and methanol–water, each with five proportions (10, 30, 50, 70 and 90%, v/v), were investigated. Samples of the washed supernatants were withdrawn and analyzed by HPLC. Second, the effect of gradient pH (5.7, 6.2, 6.8, 7.4 and 8.0) of PBS was studied. Third, different incubation time (5, 10, 20, 30 and 40 min) were investigated. Fourth, different ion strengths of the incubation buffer PBS (10, 50, 100, 200, 500 and 1000 mM) were studied. Finally, gradient incubation temperatures (20, 25, 30, 37 and 45 °C) were investigated.

Validation of the established approach

Chromatographic separation was carried out on a reversed-phase XBridge-C_{18} analytical column (250 mm × 4.6 mm, 5 μm, Waters) with the column temperature set at 30 °C. The mobile phase consisted of 10 mM ammonium acetate solution with pH adjusted to 3.5 by formic acid (A) and acetonitrile (B). A gradient program was used according to the following profile: 0–45 min, 10–100% B; 45–60 min, 100% B. The flow rate was 1 mL min^{-1}, and the injection volume was 20 μL. The UV spectra were acquired at 280 nm.

The specificity of the method was determined by analyzing AChE non-binder (caffeic acid) for interference at the retention times of the AChE binder (coptisine). Specificity was assessed by comparing the peak of coptisine to that in a solution spiked with analyte at 0.1 mg mL^{-1} for coptisine and caffeic acid. The AChE immobilized zeolites based solid-phase extraction was carried out as described above. The calibration curves were constructed by plotting the peak area of coptisine to its gradient concentrations (0.002–1 mg mL^{-1}) on the basis of linear regression model. Lower limit of quantification (LLOQ) was defined as the lowest analytical concentration on the calibration curve, which generated S/N ratios of about 10. The accuracy and precision of the method were evaluated by repeated analyses of QC samples (0.016 mg mL^{-1} for coptisine) on three consecutive days. The measured precision was expressed as relative standard deviation (R.S.D.), and the accuracy was expressed as relative error (R.E.). Matrix effects were investigated on crude extract of *Corydalis yanhusuo*, by calculating the ratio of the peak area of coptisine in the presence of crude extract of *Corydalis yanhusuo* to the peak area in absence of crude extract of *Corydalis yanhusuo* at three different QC concentrations (low, medium, and high).

Reusability of AChE immobilized zeolite and AChE conjugated magnetic nanoparticles

The reusability of AChE immobilized zeolite and AChE conjugated magnetic nanoparticles was evaluated by conducting the solid-phase extraction after incubating with coptisine at the same conditions for ten consecutive times. The AChE immobilized zeolite and AChE conjugated magnetic nanoparticles were reused after rinsed with phosphate buffer solution thoroughly. The fifth eluents of the ten consecutive cycles were collected and analyzed using HPLC-UV.

Applications to crude extract of *Corydalis yanhusuo*

The crude extract of *Corydalis yanhusuo* was characterized using ultra-high performance liquid chromatography coupled with Q-TOF 5600-plus mass spectrometer. The acquisition parameters for UPLC-Q-TOF/MS analysis were as follows: collision gas, ultrahigh-purity helium (He); nebulizing gas, high-purity nitrogen (N_2); ion spray voltage, −4.5 kV; sheath gas (N_2), 30 arbitrary units; auxiliary gas (N_2), 10 arbitrary units; capillary temperature, 350 °C; capillary voltage, −15 V; tube lens offset voltage, −30 V; and mass range, *m*/*z* 100–1500.

AChE immobilized zeolites based solid-phase extraction was performed according to the above procedure. Briefly, 20 μL aliquots of crude extract of *Corydalis yanhusuo* was incubated with 0.025 mg AChE immobilized zeolites in a total volume of 200 μL PBS buffer (10 mM, pH 7.4). After incubation at 37 °C for 20 min, AChE immobilized zeolites were washed four times with 200 μL of the PBS buffer and the supernatants were abandoned. The AChE immobilized zeolites were subsequently incubated in 20 μL of 50% (v/v) methanol/water for 10 min to dissociate specific bound compounds and the eluate was collected and analyzed *via* UPLC-Q-TOF/MS. Denatured AChE immobilized zeolites and blank zeolites were used as control to exclude the nonspecific binding.

AChE conjugated magnetic nanoparticles based solid-phase extraction was performed as below. The reaction mixtures of the crude extract of *Corydalis yanhusuo* (20 μL) and AChE conjugated magnetic nanoparticles (0.045 mg) were prepared in phosphate buffer solution to reach a final volume of 200 μL, and incubated for 20 min at 37 °C using water bath. The AChE conjugated magnetic nanoparticles were washed four times with 200 μL of the buffer. Finally, the magnetic nanoparticles were subsequently incubated in 20 μL of 50% (v/v) methanol/water for 10 min to disclose specific bound compounds. The eluate was collected and retained for analysis *via* UPLC-Q-TOF-MS.

AChE inhibitory assay

The inhibitory effects of compounds against AChE were evaluated as previously described but with minor modifications.[15] Twenty microliters of the sample solution dissolved in Tris buffer (pH 7.8) and 20 μL of the enzyme solution (0.5 U mL^{-1}) were mixed in the well of a microtiter plate. Then, 100 μL of Tris buffer (pH 7.8) were added to each well. After incubation at 37 °C for 15 min, forty microliters of 5,5′-dithiobis(2-nitrobenzoic acid) solution (0.75 mM) and 20 μL of 1.5 mM acetylthiocholine were added to initiate the enzyme reaction. On account of the hydrolysis of acetylthiocholine, yellow 5-thio-2-nitrobenzoate anion was generated, and the absorbance was recorded at a wavelength of 406 nm after incubation at 37 °C for 30 min. Galantamine was employed as the positive control. The percentage inhibition was evaluated using the equation $I(\%) = [1 - (A_{sample} - A_{background})/A_{blank}] \times 100\%$, where A_{sample} is the absorbance of each test compound, $A_{background}$ is the absorbance of the background without enzyme, and A_{blank} is the absorbance of the blank without test compound.

Published on 11 October 2016. Downloaded by Fail Open on 7/23/2025 9:11:32 AM.

Results and discussion

Characterization of AChE immobilized zeolites and AChE conjugated magnetic nanoparticles

Zeolites had been widely used and were of great interest to us. Zeolite properties can influence the protein adsorption, including zeolite structure, the chemical composition of the crystalline framework, the crystal morphology and size. Fig. S2† shows X-ray diffractograms for zeolite beta, zeolite ZSM-5 and zeolite Y, respectively, and they reveal the preparation of pure BEA-, MFI- and FAU-type zeolite structures.[11] The TEM image of control (zeolite beta without AChE) and AChE adsorbed zeolite beta was included in Fig. 2. The frame of zeolite beta without AChE was clear, whereas the zeolite became blurred after AChE adsorption. The IR spectra of zeolite beta as a control were shown in Fig. S3A.† The major IR bands of zeolite beta are 1200, 1160, 1050 and 780 cm^{-1}. Three IR bands called amide I, amide II and amide III have been used in the literature to analyze the protein structure. As was displayed in Fig. S3B,† the amide I, amide II and amide III bands in native AChE are centered at 1640, 1520 and 1250 cm^{-1}, respectively. As was shown in Fig. S3C,† the infrared spectra of adsorbed AChE on zeolite crystals reveal that there was an increase in the amide I band at 1640 cm^{-1}. No significant changes in either peak position or their relative intensities were observed after adsorption, suggesting that the protein conformation and orientation remains unvaried.

TEM image of magnetic nanoparticles revealed an average diameter of 300 nm (see Fig. S4†). The close-up of the AChE conjugated magnetic nanoparticles was present in Fig. S4B.† The red arrows clearly shows the presence of thin gray film on the surface of the AChE conjugated magnetic nanoparticles, indicating AChE was successfully conjugated onto the surface of magnetic nanoparticles. The main peaks of the X-ray diffraction of the magnetic nanoparticles, such as 2.9706, 2.5322, 2.1008, 1.7122, 1.6146 and 1.4837, matched well with the standard magnetite Fe_3O_4 XRD spectrum (see Fig. S5†). Magnetization curves of blank magnetic nanoparticles (black) and AChE conjugated magnetic nanoparticles (red) were shown in Fig. S6.† Maximum saturation magnetization (50.2 emu g^{-1}) of AChE conjugated magnetic nanoparticles is a little less than that (79.4 emu g^{-1}) of blank magnetic nanoparticles due to the nonmagnetic AChE on the surface. The amounts of magnetic nanoparticles were varied to determine the optimal ratio for AChE binding efficacy with a constant amount of AChE. As shown in Fig. S7,† with increasing the amount of Fe_3O_4 added at a constant tyrosinase amount of 100 μg, the amount of tyrosinase bound gradually increased and then reached a plateau (~99%) when the amount of Fe_3O_4 added was above 175 μL. The results suggested that a ratio of 175 μL Fe_3O_4 per 100 μg tyrosinase was sufficient for immobilization.

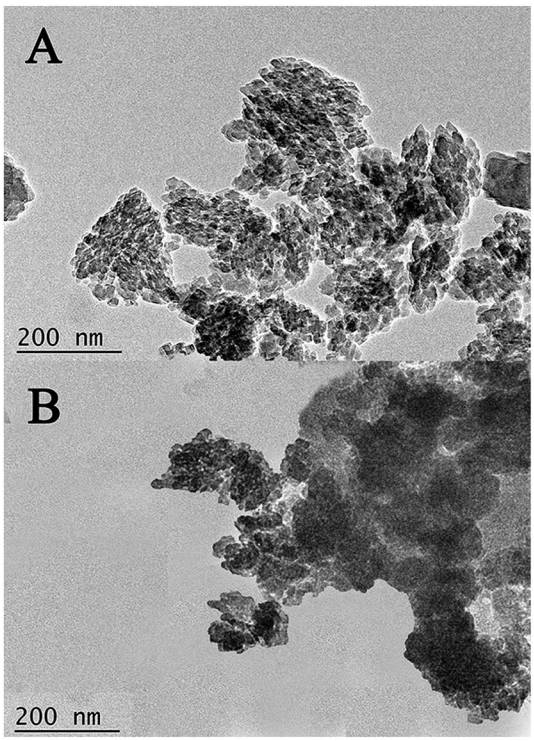

Fig. 2 TEM images of blank zeolite beta (A) and AChE immobilized zeolite beta (B).

Optimization conditions for AChE immobilization

Four parameters of the adsorption procedure were investigated, including different kinds of zeolites, adsorption time, buffer pH and temperature. The initial trend of the curves obtained for the microporous crystals has a very fast adsorption. When the time is prolonged, the amount of adsorbed protein increases slowly (see Fig. S8A†). The percentage of adsorbed AChE for three kinds of zeolites reached a plateau after 45 min of adsorption. Moreover, the largest percentage of adsorbed AChE was achieved by using zeolite beta as adsorbent (about 88%). The final protein–zeolite ratio was 1.76 : 1. Therefore, zeolite beta was employed for the next experiment.

The effect of pH values of the incubation buffer was also investigated. The variation in buffer pH from 5.7 to 7.4 increased the percentage of adsorbed AChE from 86.7% to 91.8%. The difference was statistically significant (see Fig. S8B†). The influence of temperatures on the adsorption was studied and the result was presented in Fig. S8C.† The highest percentage of adsorbed AChE was achieved when the incubation temperature was set to 26 °C. In summary, the optimal conditions of AChE adsorption were as follows: adsorption support: zeolite beta; incubation pH: 6.2; incubation temperature: 26 °C.

Desorption of AChE from zeolites was performed by addition of 0.2 M NaOH solutions to the AChE adsorbed zeolite. The mixture of NaOH solution and zeolite-adsorbed fraction was incubated for 45 min at 37 °C. Supernatant was obtained by flash spin down at 12 000 rpm for several seconds. Concentration of desorbed AChE in supernatant was determined by Bradford method. The time-desorption ratio curve was shown in Fig. S9.† About 90% desorption was achieved after 15 min's desorption. Further increase the incubation time didn't lead to the increase of desorption ratio. Meanwhile, the activity of

 This journal is © The Royal Society of Chemistry 2016

Published on 11 October 2016. Downloaded by Fail Open on 7/23/2025 9:11:32 AM.

recovered protein powder was comparable with that of original protein powder by incubation with the substrate.

The type of possible interactions between zeolites and AChE are complicated. Since the zeolite structures have microporous pores which are too small with respect to the kinetic diameter of the AChE, the adsorption occurs solely on the external crystalline surface. They could consist in acid–base reactions between the amino groups of the protein and the surface hydroxyl groups of the zeolites (silanol groups) or van der Waals or electrostatic interactions. The schematic illustration of the possible mechanism of adsorption and desorption behavior of the AChE on zeolite beta were shown in Fig. S10.† AChE was comprised of basic amino and acidic carboxyl functional groups as well as a characteristic side chain. The amino and carboxyl groups give the enzyme unusual electrolytic properties. At high pH, the carboxyl group tends to be dissociated, giving the compound a negative charge. At low pH, the amino group, as well as the overall molecule, becomes positively charged. At an interim pH known as the isoelectric point, enzyme in solution has a net charge of zero. The isoelectric point of AChE was about 7.5. As shown in Fig. S8,† the optimal pH for adsorption was determined to be 6.2, which was below the isoelectric point of AChE. The net charge of AChE was positive. It may substitute the positive charged H^+ sites in the H-type zeolite beta. After immersed into NaOH solution, the positive charged AChE was neutralized and dissociated from the zeolite. Na^+ ion may take the place of AChE on zeolite. In summary, electrostatic interactions play the pivotal role in the adsorption and desorption behavior of AChE onto the zeolite.

Optimization conditions for AChE immobilized zeolites based solid-phase extraction

The washing step after incubation is of great importance in solid-phase extraction of binders using AChE immobilized zeolites, because unbound or nonspecific compounds may interfere with the result. Investigations of different washing times (1–5 times) were performed. As was shown in Fig. S11A,† four times of washing was adequate for removing any unbound compounds. The peak area of coptisine was almost zero in the eluent of fourth wash, indicating that all nonspecific binding coptisine had been completely washed out by four times wash. A denaturing solvent was used to denature the AChE and dislodge the specially bound compound. Two-solvent systems (acetonitrile–water and methanol–water), each with five proportions (10, 30, 50, 70 and 90%, v/v), were evaluated. As shown in Fig. S11B,† the extraction efficiency of coptisine washed by 50% (v/v) methanol–water was the largest. Therefore, 50% (v/v) methanol–water was chosen as denaturing solvent.

The pH of a solution can have several effects on the structure and activity of enzymes. Changes in pH may not only affect the shape of an enzyme but it may also change the shape or charge properties of the substrate so that either the substrate cannot bind to the active site or it cannot undergo catalysis. In general, enzyme has a pH optimum. The isoelectric point of AChE was 7.5 and the pK_a value of coptisine was 10.7. AChE was negative charged within the pH range 5.7–7.5, while coptisine was positive charged within the pH range 7.5–8.0. The electrostatic attraction between AChE and coptisine increased when the pH gradually increased. As was shown in Fig. S12A,† the largest binding degree of coptisine was achieved at pH around 7.4.

The length of incubation time is a factor affecting the binding degree. As was shown in Fig. S12B,† the optimum incubation time was about 20 min. Further increase of the incubation time led to unfavorable binding, indicating that the active site of AChE had already been saturated with coptisine after 20 min' incubation. Therefore, 20 min was selected as the length of incubation time.

The total ion concentration in solution will affect important properties such as the distribution of charge on exterior surfaces of enzyme, in addition to the reactivity of the catalytically active groups. As was shown in Fig. S12C,† the increasing in the PBS concentration from 10 mM to 1000 mM led to the decrease in the bound ratio of coptisine. This phenomenon may be explained by the fact that the surface charge of AChE was neutralized by excessive PBS, which led to a significant decrease in the electrostatic interaction between coptisine and AChE. Thus, PBS concentration of 10 mM was chosen in this experiment.

Enzymes are catalysts and act to reduce the amount of activation energy required for a reaction to occur. Raising the temperature will reduce the amount of required activation energy allows for the reaction to occur, but also may denature an enzyme so that it is no longer functional. Lowering the temperature will reduce the rate of the reaction so low as to make it seem non-functional. In general, enzyme has a temperature optimum. As was shown in Fig. S12D,† the optimum temperature was about 37 °C due to the largest binding degree at this temperature.

Collectively, the optimal AChE immobilized zeolite based solid-phase extraction conditions were as follows: pH value: 7.4, incubation time: 20 min, ion strength: 10 mM, temperature: 37 °C.

Validation of the established approach

The aim of this section was to investigate the interference of nuisance compounds or by the synergistic effects of several other compounds and ensure the result of the approach was reliable. Coptisine, is a well-known AChE inhibitor, which belongs to alkaloids.[14] Caffeic acid, which is a phenolic compound, displays negative AChE inhibitory effect. Thus, coptisine and caffeic acid were chosen to investigate the specificity of the zeolite based solid-phase extraction approach. As

Table 1 Recovery of coptisine in crude extract of *Corydalis yanhusuo*

Sample	Initial (μM)	Added concentration (μM)	Found concentration (μM)	Recovery (%)	RSD (%)
Crude extract	166.47	195.12	366.55	103	2.2
		780.47	974.99	104	0.9
		1560.49	1811.96	105	0.7

Published on 11 October 2016. Downloaded by Fail Open on 7/23/2025 9:11:32 AM.

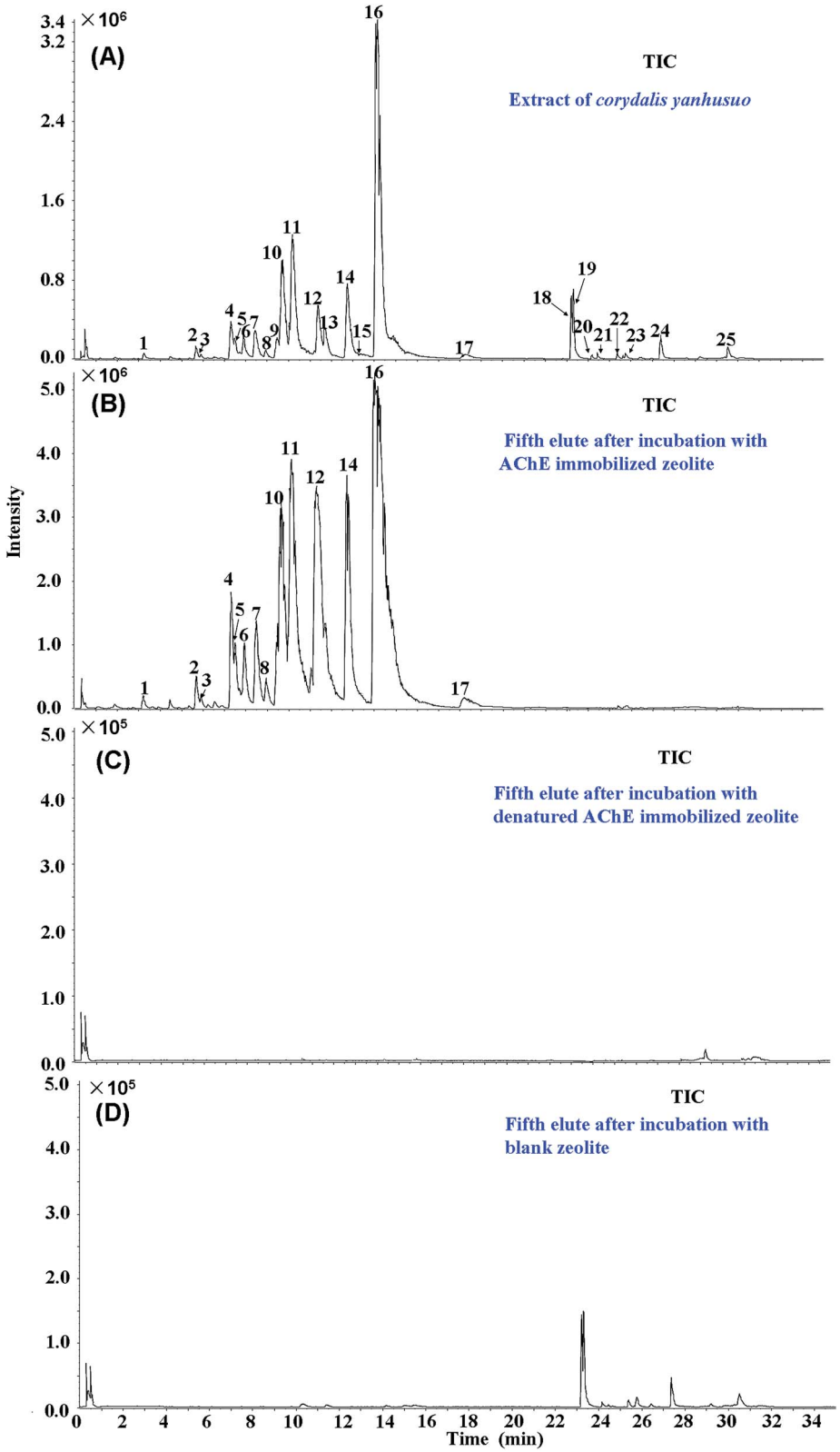

Fig. 3 TIC chromatograms of (A) crude extract of *Corydalis yanhusuo*, (B) fifth eluent after incubation with AChE immobilized zeolite beta, (C) fifth eluent after incubation with denatured AChE immobilized zeolite beta, (D) fifth eluent after incubation with blank zeolite beta.

was shown in Fig. S13A,† the peak of coptisine was observed in the presence of caffeic acid (see black line and red line) after zeolite based solid-phase extraction, indicating that the method had good specificity with no interference of the inactive compound caffeic acid. To avoid the nonspecific binding, denatured AChE immobilized zeolites was used to be incubated

 This journal is © The Royal Society of Chemistry 2016

Published on 11 October 2016. Downloaded by Fail Open on 7/23/2025 9:11:32 AM.

with the mixture of coptisine and caffeic acid. None of the unspecific binding was observed (see red line in Fig. S13B†).

The calibration curve, linear range, LLOD, LLOQ, and repeatability of coptisine were performed using the developed approach. Reasonable correlation coefficient values (r^2 = 0.9977) showed good correlations between coptisine concentrations and its peak area within the ranges tested. The LLOD and LLOQ for coptisine were determined as 0.293 μg mL^{-1} and 0.488 μg mL^{-1}, respectively. The repeatability present as RSD (n = 6) was 0.99%. The overall intra- and inter-day variations (RSD) of coptisine were 0.98% and 3.79%, respectively. The developed approach showed good accuracy with the recoveries ranging from 103% and 105% (see Table 1). As shown in Fig. S14,† the activity of AChE immobilized zeolite retained 89% after ten cycles. Reusability can decrease the test costs and enhance the experimental efficiency. Collectively, the results demonstrated that the method was sensitive, precise, and accurate enough for zeolites based solid-phase extraction of AChE binders.

Applications to extracts of crude extract of *Corydalis yanhusuo*

The optimized UPLC-Q-TOF-MS protocol was employed for the separation and identification of compounds in crude extract of *Corydalis yanhusuo*. The total ion current chromatograms were shown in Fig. 3A. A total of twenty-five compounds were characterized, including 16 alkaloids, 3 sphingolipids and 6 unknowns, and their detailed information was presented in Table 2. The retention time and fragmentation information of compounds **4**, **7**, **9**, **10**, **11**, **12**, **14**, **15** and **16** were compared with that of standard compounds (see Fig. S15†). Chemical structures of the identified compounds were shown in Fig. S16.†

The developed AChE immobilized zeolites based solid-phase extraction approach was applied to the crude extract of *Corydalis yanhusuo* and the results were shown (see Fig. 3B–D). Compound **1–8**, **10–12**, **14**, **16** and **17** were the AChE binders identified from crude extract of *Corydalis yanhusuo*. The AChE conjugated magnetic nanoparticles based solid-phase extraction approach was also used to extract binders from the crude extract of *Corydalis yanhusuo* and the results were displayed in

Table 2 MS^1 and MS^2 data of constituents in crude extract of *Corydalis yanhusuo* using UPLC-Q-TOF-MS

				ESI-MS(+)			
No.	t_R (min)	MS^2	Formula	Measured mass $[M]^+$ or $[M+H]^+$	Error (ppm)	Identification	Structure type
1	3.261	**177.0549**, 145.0285	$C_{17}H_{23}NO_4$	307.1771	−2.3	Unknown	—
2	5.674	271.1339, 269.1186, 237.0911, 209.0966, 175.0750, 143.0491, **107.0495**	$C_{19}H_{23}NO_3$	314.1760	3.0	Armepavine	I
3	5.902	**178.0869**, 163.0628	$C_{19}H_{21}NO_4$	328.1554	3.2	Scoulerine	IV
4[a]	7.314	**178.0867**, 163.0627	$C_{20}H_{23}NO_4$	342.1710	3.0	Tetrahydrocolumbamine	IV
5	7.504	341.1634, **192.1023**, 177.0787	$C_{21}H_{25}NO_4$	356.1866	2.7	Glaucine	V
6	7.911	341.1638, **192.1026**, 177.0790	$C_{21}H_{25}NO_4$	356.1865	2.4	Glaucine isomer	V
7[a]	8.448	336.1249, 275.0716, 247.0764, 206.0820, 189.0787, **188.0712**, 149.0600	$C_{20}H_{19}NO_5$	354.1348	3.4	Protopine	II
8	8.933	341.1641, 192.1026, **178.0867**, 163.0633, 151.0765	$C_{21}H_{25}NO_4$	356.1867	3.0	Isocorybulbine	IV
9[a]	9.463	352.1561, 290.0953, 206.0820, 189.0789, **188.0714**	$C_{21}H_{23}NO_5$	370.1662	3.5	Allocryptopine	II
10[a]	9.722	325.1447, 310.1208, 295.0983, 294.1255, 279.1023, **192.1015**, 176.0708, 165.0910	$C_{21}H_{25}NO_4$	356.1868	3.3	Tetrahydropalmatine	IV
11[a]	10.240	**292.0977**, 277.0747, 262.0874	$C_{19}H_{14}NO_4$	320.0928	3.3	Coptisine	III
12[a]	11.410	354.1716, **192.1020**, 165.0912	$C_{22}H_{27}NO_4$	370.2026	3.6	Corydaline	IV
13	11.706	**337.1326**, 336.1245, 322.1094, 308.1298, 294.1142, 293.1063	$C_{21}H_{22}NO_4$	352.1555	3.3	Dehydrocorybulbine	III
14[a]	12.782	337.1325, **336.1239**, 322.1090, 308.1293, 294.1138, 292.0958	$C_{21}H_{22}NO_4$	352.1558	4.2	Palmatine	III
15[a]	13.078	321.1017, **320.0936**, 306.0775, 304.0988, 292.0984, 278.0823	$C_{20}H_{18}NO_4$	336.1243	3.8	Berberine	III
16[a]	14.133	**350.1406**, 336.1252, 322.1454, 308.1300, 306.1150	$C_{22}H_{24}NO_4$	366.1714	3.9	Dehydrocorydaline	III
17	18.223	337.0968, 322.0737, **306.0781**	$C_{20}H_{18}NO_5$	352.1199	5.5	Berberastine	III
18	23.192	**256.2649**, 106.0869, 102.0920, 88.0766, 70.0667	$C_{16}H_{35}NO_2$	274.2752	4.2	Hexadecasphinganine	VI
19	23.340	300.2914, **256.2638**, 102.0919, 88.0764, 70.0665	$C_{18}H_{39}NO_3$	318.3020	5.4	Phytosphingosine	VI
20	24.184	425.2209, **379.2231**, 249.1446	$C_{22}H_{28}O_{10}$	453.1699	0.6	Unknown	—
21	24.455	**284.2956**, 106.0865, 88.0762	$C_{18}H_{39}NO_2$	302.3064	3.5	Sphinganine	VI
22	25.386	212.2378, **91.0544**, 58.0670	$C_{21}H_{38}N$	304.3010	3.7	Unknown	—
23	25.765	—	$C_{27}H_{36}O_7$	473.2534	0.0	Unknown	—
24	27.431	—	$C_{25}H_{28}O_7$	441.1913	1.2	Unknown	—
25	30.538	321.3172, 303.3060, 163.1484, 149.1325, 135.1170, 97.1012, 83.0863	$C_{22}H_{44}NO$	338.3433	3.0	Unknown	—

[a] Compared to standard compounds, I: benzylisoquinoline alkaloid; II: protopine-type alkaloids; III: protoberberine-type alkaloids; IV: tetrahydroprotoberberine-type alkaloids; V: aporphine-alkaloids; VI: sphingolipid.

Published on 11 October 2016. Downloaded by Fail Open on 7/23/2025 9:11:32 AM.

Fig. 4. Compounds **4**, **6–12**, **14** and **16** were identified as AChE binders. A Venn diagram was generated for demonstrating commonly and exclusively detected AChE binders by using the two solid-phase extraction approaches (see Fig. S17†). Nine compounds, including tetrahydrocolumbamine, glaucine isomer, protopine, isocorybulbine, tetrahydropalmatine, coptisine, corydaline, palmatine, dehydrocorydaline, were the common AChE binders identified.

Compound **2** showed the $[M + H]^+$ ion at *m/z* 314 and produced characteristic ions at *m/z* 107 and 206 in MS^2 spectrum, which were formed by inductive cleavage and α-cleavage at the nitrogen of the tyramine moiety. Compared with the literature,[16] compound **2** was tentatively deduced as armepavine. Aporphine alkaloids do not undergo the RDA reaction and are thus easily distinguished from the protopine and tetrahydroprotopine alkaloids. The retro-Diels–Alder (RDA) reaction is a characteristic fragmentation pathway of the tetrahydroprotoberberine. Compound **4** displayed $[M + H]^+$ ion at *m/z* 342 and yielded the predominant product ions at *m/z* 178 and 163, corresponding to the RDA C-ring opening and loss of a methyl group (see Fig. S18A†). Compounds **3** and **4** gave the same product ions at *m/z* 178 and 163, but compound **3** showed an decrease of 14 Da of the corresponding $[M]^+$ compared to compound **4**, Meanwhile, compound **3** had an earlier retention time. Compared with the literature,[16] compounds **3** and **4** were tentatively identified as scoulerine and tetrahydrocolumbamine. Compound **5** showed $[M + H]^+$ ion at *m/z* 356 and gave the predominant product ions at *m/z* 192 and 177, which resulted from RDA C-ring opening and loss of a methyl group (see Fig. S18B†). Compound **5** was tentatively identified as glaucine. Compounds **6**, **8** and **5** shared the same $[M + H]^+$ ion at *m/z* 356 and produced the same fragment ions at *m/z* 341 and 192 (see Fig. S19A†). Considering the retention time of the three compounds, compound **6** and **8** were plausibly deduced as glaucine isomer and isocorybulbine.[17]

Common characteristic product ions of protopine-type alkaloids were yielded by various dissociation processes such as retro-Diels–Alder (RDA) fragmentation, dehydration, and successive dissociation of substitute groups in MS^2 spectrum.[17] Compounds **7** and **9** showed the $[M + H]^+$ ions at *m/z* 354 and 370, respectively (see Fig. S18C†). Compared with the standards, compounds **7** and **9** were characterized as protopine and allocryptopine, respectively. Two compounds shared common characteristic ions at *m/z* 206, 189, and 188, which were produced by retro-Diels–Alder (RDA) fragmentations and the loss of H_2O and hydroxyl group, respectively. The neutral loss of H_2O led to product ions at *m/z* 336 of compound **7** and *m/z* 352 of compound **9** in MS^2 spectrum. Compound **10** showed $[M + H]^+$ ion at *m/z* 356 and produced characteristic ions at *m/z* 325, 310, 295, 279 in MS^2 spectrum (see Fig. S19B†), which corresponded to the loss of a methoxy radical, one methyl radicals, two methyl radicals and a methoxy radical. Based on the above information, compound **10** was plausibly assigned as tetrahydropalmatine.

The characteristic product ions of protoberberine-type alkaloids were yielded by the successive cleavage of substituted groups of methyl, CO radical on the A- and D-rings.[17] No RDA fragmentation occurs due to that it was difficult to open the ring. Compound **12** displayed $[M + H]^+$ ion at *m/z* 370 and yielded the fragment ions at *m/z* 354, 192 and 165, which

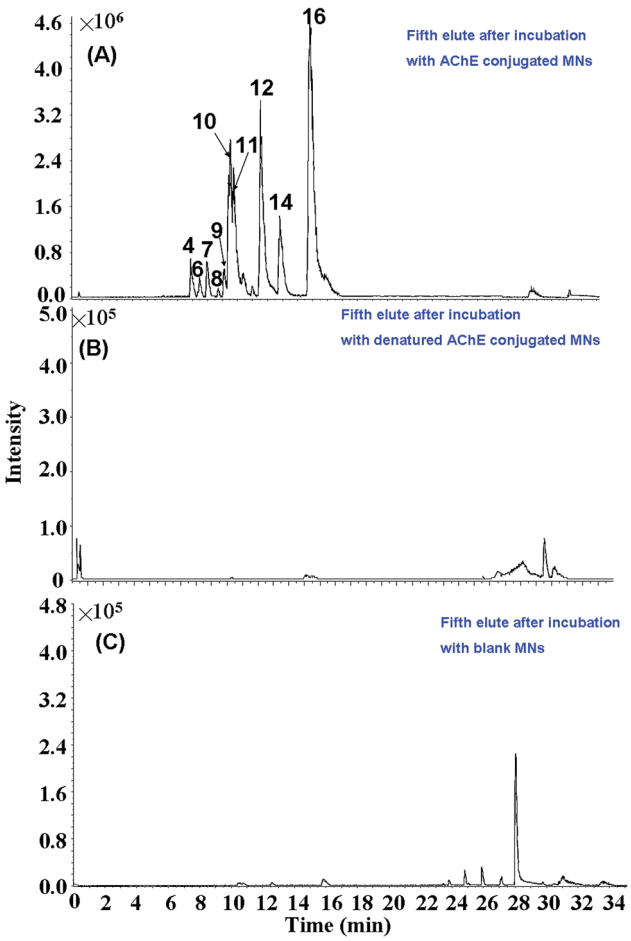

Fig. 4 TIC chromatograms of (A) fifth eluent after incubation with AChE conjugated magnetic nanoparticles; (B) fifth eluent after incubation with denatured AChE conjugated magnetic nanoparticles, (C) fifth eluent after incubation with blank magnetic nanoparticles.

Table 3 Inhibitory effects of compounds on acetylcholinesterase activities

No.	Compound	IC_{50} (μM) ± SD
4	Tetrahydrocolumbamine	136.20 ± 2.77
7	Protopine	128.55 ± 3.91
9	Allocryptopine	104.48 ± 2.02
10	Tetrahydropalmatine	137.16 ± 3.19
11	Coptisine	4.40 ± 0.12
12	Corydaline	241.61 ± 21.37
14	Palmatine chloride	0.64 ± 0.00
15	Berberine	26.60 ± 0.50
16	Dehydrocorydaline	10.13 ± 0.07
	Columbamine	47.14 ± 0.57
	Tetrahydrocoptisine	167.27 ± 4.58
	Corynoline	198.67 ± 3.24
	Dehydroglaucine	119.84 ± 3.12
	Tetrahydroberberine	60.95 ± 3.54
Control	Galantamine	3.48 ± 0.02

This journal is © The Royal Society of Chemistry 2016

Published on 11 October 2016. Downloaded by Fail Open on 7/23/2025 9:11:32 AM.

Table 4 A comparison between zeolite and magnetic nanoparticles based solid-phase extraction approaches

Method	Zeolite based SPE method	Magnetic beads based SPE method
Enzyme immobilization mode	Adsorption	Covalent bonding
Protein–material amount ratio (mg mg^{-1})	1.76 : 1	0.57 : 1
Activity of the enzyme	Function	Function
Reusability	Yes	Yes
Regeneration	Yes (desorption)	No
Environmentally friendly	Yes	No
Cost	Cheap	Cheap

resulted from loss of CH_2 group, RDA C-ring opening and rearranged RDA reactions. Thus, compound **12** was deduced as corydaline.[18] Compounds **11** and **14–16** were identified as coptisine, palmatine, berberine and dehydrocorydaline and validated with reference standards. For instance, compound **16** showed $[M]^+$ ions at *m/z* 354 and yielded fragment ions at *m/z* 350, 336, 322, and 308, corresponding to $[M - CH_3 - H]^+$, $[M - 2CH_3]^+$, $[M - CH_3 - H - CO]^+$, and $[M - 2CH_3 - CO]^+$. Compared with the literature,[19] compound **16** was unambiguously deduced as dehydrocorydaline. Compounds **13** and **14** shared the same $[M]^+$ ion at *m/z* 354 and produced the same fragment ions at *m/z* 336, 322, and 308 (see Fig. S19C†). Compounds **13** and **14** were structural isomers. Compared with the standard, compound **14** was unambiguously identified as palmatine. Compound **13** was tentatively deduced as dehydrocorybulbine in comparison with the literature.[19]

AChE inhibitory assay

According to the previous result, compounds **1–12**, **14**, **16** and **17** should be evaluated for their inhibitory effect against AChE. However, due to the lack of standard compounds, the inhibitory effects of **1–3**, **5–6**, **8** and **13** were not well elucidated at present. In the future, their inhibitory effects will undoubtedly be elucidated with the endeavor of phytochemistry research. Therefore, fourteen compounds were obtained and evaluated for their inhibitory activities against AChE using AChE inhibitory assay. Galantamine served as the positive control. The IC_{50} value of galantamine was determined to be 3.48 μM, which was in agreement with the report in the reference.[15]

The assay results of other compounds were presented in Table 3. Palmatine chloride, exhibited the best AChE inhibitory activity with an IC_{50} value of 0.64 μM. Coptisine showed a comparable inhibitory effect with that of galantamine with an IC_{50} value of 4.40 μM. The AChE inhibitory activities of other alkaloids were decreased in the following order: dehydrocorydaline, berberine, columbamine, tetrahydroberberine, allocryptopine, dehydroglaucine, protopine, tetrahydrocolumbamine, tetrahydropalmatine, tetrahydrocoptisine, corynoline and corydaline. The AChE inhibitory effect of columbamine, coptisine, palmatine and berberine had been reported before.[14] The AChE inhibitory effects of dehydrocorydaline, allocryptopine, corydaline dehydroglaucine, protopine, tetrahydrocoptisine, tetrahydropalmatine, corynoline, tetrahydro-columbamne and tetrahydroberberine were reported for the first time.

Comparisons of the two SPE methods

A comparison between zeolite and magnetic nanoparticles based solid-phase extraction approaches were summarized in Table 4. First, the enzyme immobilization modes of the two SPE methods were different. Adsorption is the immobilization mode for zeolite based SPE method, whereas covalent bonding is the immobilization mode for magnetic nanoparticles based SPE method. Second, the AChE–zeolite immobilization ratio of was three times larger than that of AChE–magnetic nanoparticles, which meant more AChE could be immobilized onto the same amount of zeolite. Third, both of AChE immobilized zeolites and AChE conjugated magnetic nanoparticles could be reused, however, AChE can be recycled from the zeolites by desorption. If the enzyme is expensive, the recycled property of AChE immobilized zeolites is very useful. Fourth, AChE immobilized zeolites based SPE method only requires AChE and zeolite, which is environmentally friendly, while AChE conjugated magnetic nanoparticles based SPE method need glutaraldehyde, which is toxic and a strong irritant. Finally, the cost of the two SPE methods is low.

Conclusions

In the current, a new zeolite based solid-phase extraction approach in combination with UPLC-Q-TOF-MS had been established for identifying AChE binders from crude extract of *Corydalis yanhusuo*. AChE can be recycled from the zeolites by desorption. The new approach was convenient, sensitive, precise and environmentally friendly, which served as an alternative to the traditional methods for discovering anti-AChE agents from the extracts of crude drugs. Notably, fourteen AChE inhibitors were identified, ten of which were reported for the first time.

Acknowledgements

This study was supported by the Natural Science Foundation for the Youth of Jiangsu Province (No. BK20140963), the Nutritional Science Foundation of By-Health Co. (No. TY0141103) and the Priority Academic Program Development of Jiangsu Higher Education Institution (PAPD).

Published on 11 October 2016. Downloaded by Fail Open on 7/23/2025 9:11:32 AM.

References

1 P. Devos, N. Haeffner-Cavaillon, S. Ledoux, C. Balandier and J. Menard, *Lancet*, 2014, **383**, 1805.
2 K. Whalley, *Nat. Rev. Drug Discovery*, 2014, **13**, 887.
3 J. Ou, L. Kong, C. Pan, X. Su, X. Lei and H. Zou, *J. Chromatogr. A*, 2006, **1117**, 163–169.
4 J. Zhang, Y. Jin, J. Dong, Y. Xiao, J. Feng, X. Xue, X. Zhang and X. Liang, *Talanta*, 2009, **78**, 513–522.
5 A. Adsersen, B. Gauguin, L. Gudiksen and A. K. Jäger, *J. Ethnopharmacol.*, 2006, **104**, 418–422.
6 S. Radhakrishnan, P. J. Goossens, P. C. Magusin, S. P. Sree, C. Detavernier, E. Breynaert, C. Martineau, F. Taulelle and J. A. Martens, *J. Am. Chem. Soc.*, 2016, **138**, 2802–2808.
7 J. Shi, Y. Wang, W. Yang, Y. Tang and Z. Xie, *Chem. Soc. Rev.*, 2015, **44**, 8877–8903.
8 T. Willhammar, J. Sun, W. Wan, P. Oleynikov, D. Zhang, X. Zou, M. Moliner, J. Gonzalez, C. Martínez, F. Rey and A. Corma, *Nat. Chem.*, 2012, **4**, 188–194.
9 M. Hernandez-Rodriguez, J. L. Jorda, F. Rey and A. Corma, *J. Am. Chem. Soc.*, 2012, **134**, 13232–13235.
10 M. R. Hudson, W. L. Queen, J. A. Mason, D. W. Fickel, R. F. Lobo and C. M. Brown, *J. Am. Chem. Soc.*, 2012, **134**, 1970–1973.
11 A. Tavolaro, P. Tavolaro and E. Drioli, *Colloids Surf., B*, 2007, **55**, 67–76.
12 J. E. Krohn and M. Tsapatsis, *Langmuir*, 2005, **21**, 8743–8750.
13 M. Matsui, Y. Kiyozumi, Y. Mizushina, K. Sakaguchi and F. Mizukami, *Sep. Purif. Technol.*, 2015, **149**, 103–109.
14 H. Zhao, S. Zhou, M. Zhang, J. Feng, S. Wang, D. Wang, Y. Geng and X. Wang, *J. Pharm. Biomed. Anal.*, 2016, **120**, 235–240.
15 L. Cahlikova, D. I. Perez, S. Stepankova, J. Chlebek, M. Safratova, A. Host'alkova and L. Opletal, *J. Nat. Prod.*, 2015, **78**, 1189–1192.
16 F. Wang, Y. Ai, Y. Wu, W. Ma, Q. Bian, D. Y. Lee and R. Dai, *J. Sep. Sci.*, 2015, **38**, 917–924.
17 M. Sun, J. Liu, C. Lin, L. Miao and L. Lin, *Acta Pharm. Sin. B*, 2014, **4**, 208–216.
18 X. Yan, Q. Zhang and F. Feng, *J. Sep. Sci.*, 2016, **39**, 1442–1453.
19 X. H. Yang, X. L. Cheng, B. Qin, Z. Y. Cai, X. Cai, S. Liu, Q. Wang and Y. Qin, *J. Pharm. Biomed. Anal.*, 2016, **124**, 319–336.

This journal is © The Royal Society of Chemistry 2016